ChemComm

FEATURE ARTICLE

View Article Online
View Journal

Cite this: DOI: 10.1039/c7cc02592k

Towards seamlessly-integrated textile electronics: methods to coat fabrics and fibers with conducting polymers for electronic applications

Linden Allison,† Steven Hoxie† and Trisha L. Andrew *

Received 4th April 2017,
Accepted 23rd May 2017

DOI: 10.1039/c7cc02592k

rsc.li/chemcomm

Traditional textile materials can be transformed into functional electronic components upon being dyed or coated with films of intrinsically conducting polymers, such as poly(aniline), poly(pyrrole) and poly-(3,4-ethylenedioxythiophene). A variety of textile electronic devices are built from the conductive fibers and fabrics thus obtained, including: physiochemical sensors, thermoelectric fibers/fabrics, heated garments, artificial muscles and textile supercapacitors. In all these cases, electrical performance and device ruggedness is determined by the morphology of the conducting polymer active layer on the fiber or fabric substrate. Tremendous variation in active layer morphology can be observed with different coating or dyeing conditions. Here, we summarize various methods used to create fiber- and fabric-based devices and highlight the influence of the coating method on active layer morphology and device stability.

1. Introduction

Wearable electronics constitute the frontier of human interface devices that are making possible advanced performance monitoring,[1] physiochemical sensing,[2] new haptic interfaces,[3] and portable energy harvesting[4] and energy storage,[5] to name a few innovations. Most recently-reported devices can be considered as non-natural approximations of traditional textiles or threads. Many wearable devices are built on thin or ultrathin plastic substrates that display sufficient flexibility to be skin- or body-mounted, or incorporated into garments and accessories *via* patching.[6] Selected other devices are created using specialty or designer threads/fibers, which are sometimes yarned together then coated with a protective polymer cladding to yield a fiber-based electronic device.[7] To date, these devices demonstrate acceptable device metrics, but their performance and longevity is far from matching those of devices built on rigid substrates, such as glass and silicon.[5,8]

For nascent wearable technology, in particular, aesthetics and haptic perception can uniquely determine the difference between success (*i.e.*, widespread adoption) and failure, irrespective of device metrics. There is strong motivation for using substrates and scaffolds that are already familiar, such as cotton/silk thread, fabrics and clothes, and imperceptibly adapting them to a new technological application. The pliability, breathability, wearability and feel of fabrics is unmatched. Especially for skin-mountable devices and smart garments, the intrinsic breathability and feel of fabrics cannot be replicated by devices built on plastic substrates or designer fibers, no matter how thin or flexible these devices can be made. Moreover, using traditional textile materials means that prototypes of promising new technologies can be easily produced using existing manufacturing routines.

A number of research groups are endeavoring to transform familiar fibers and/or fabrics into fiber- or textile-based electrodes for electronic devices. This is usually achieved by coating or soaking (*i.e.*, dyeing) mass-produced threads or fabrics with electronically- or optoelectronically-active materials.[9] Intrinsically conducting polymers (ICPs) are typically used as the active layer materials for many fiber-and textile-based devices due to their advantageous mechanical properties and processing ease. The elasticity and plasticity of ICPs are similar to those of common, mass-produced threads, which should prevent delamination and microfissure formation within the active layer upon bending or twisting the coated/dyed threads. Nonetheless, fabrics and threads/yarns are demanding substrates onto which to deposit a conjugated polymer film because their surfaces are densely textured and display roughness over a wide range of length scales—micron length scales for fibers, micron to millimeter length scales for threads/yarns and millimeter to centimeter length scales for woven and knitted fabrics. Indeed, tremendous variation in the surface morphology of conjugated polymer-coated fibers can be observed with different coating or processing conditions.

Importantly, the morphology of the conjugated polymer active layer determines electrical performance and device ruggedness.

Department of Chemistry, University of Massachusetts Amherst, Amherst, MA 01003, USA. E-mail: tandrew@umass.edu
† These authors contributed equally.

For fiber-based devices, in particular, the stability of a particular coating against high friction forces, extreme bending radii and other large, cyclic mechanical stresses is paramount. Typical textile manufacturing processes, such as weaving, knitting and sewing, subject threads/yarns to astonishingly-high mechanical strain.[10] Further, any textiles thus produced are subjected to significant strain, friction forces and chemical exfoliation during wear, laundering, and/or ironing. To survive these stresses, electronically-active coatings must be smooth, uniform, conformal and, ideally but not necessarily, covalently-tethered to the surface of a fiber to limit exfoliation and de-adhesion events.

Here we summarize selected recent approaches to coat familiar, mass-produced threads, yarns, or fabrics with electronically-active conjugated polymers to produce textile-based electronic devices. Previous reviews have described recent advances in fiber-based photovoltaic devices[8] and textile energy storage,[5] with particular emphasis on device performance. Therefore, in this article, we place emphasis on the fabrication method used to create various fiber- and textile-based devices and attempt to highlight the influence of the coating method on active layer morphology and device stability.

2. Dipcoating

2.1 Film morphology and stability

Dipcoating or, effectively, dyeing fibers and textiles with pre-synthesized conducting polymers is the most prevalent approach for creating electronically-active textiles. This method is relatively simple and does not require specialized or expensive equipment. Dipcoating only requires that the conjugated polymer be soluble in a solvent that does not degrade the fiber or textile substrate. This allows for the fiber/textile to be simply soaked in a solution of the solubilized polymer then dried, leaving behind a conductive coating. The dipping-drying cycle can also be repeated multiple times to either systematically increase the thickness of a polymer coating or add multiple layers of different conjugated polymers. However, caution must be exercised to ensure that the fibers/fabrics are completely dry before undertaking a subsequent dipping cycle to prevent dissolution of the already-formed coating.

For example, Sonkusale and Khademhosseini *et al.* used sequential dipcoating to create a fully-integrated thread-based diagnostic device platform that contained both a thread-based microfluidic network and an array of thread-based physical and chemical sensors capable of monitoring physiochemical tissue properties *in vitro* and *in vivo* (Fig. 1).[2] The thread-based chemical sensors were fabricated by sequentially passing raw cotton yarns through multiple wells containing acidic poly(aniline) (PANI) and isopropanol-solubilized conductive carbon inks. A dryer was utilized to cure each coating in between each dipping event. Meters of functionalized threads were thus fabricated and collected on rotating spools.

A similar assembly line approach was used by Gaudiana *et al.* to fabricate fiber-based organic photovoltaic devices.[7b] The authors drew specially-extruded stainless steel threads through a sequence of vertically-aligned coating cups containing,

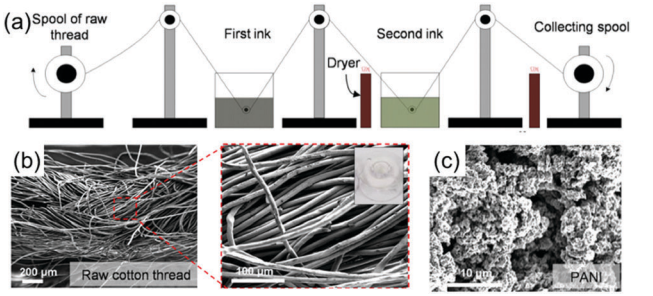

Fig. 1 (a) Sequential dipcoating process reported by Sonkusale and Khademhosseini *et al.* (b) SEMs of raw cotton thread before dipcoating. (c) SEM of poly(aniline) coated cotton thread. Adapted from ref. 2.

first, an isopropanol solution of tetrabutyl titanate, second, a semiconducting polymer-fullerene mixture in an organic solvent and, third, an aqueous solution of the highly-conductive composite material, poly(3,4-ethylenedioxythiophene)-*co*-poly(styrene sulfonic acid) (PEDOT:PSS). Here, too, a dryer was utilized to cure each coating in between each dipping event. These multiply-coated threads were then yarned together with a second, silver-coated stainless steel thread and the yarns dipcoated with a transparent protective cladding to produce fiber solar cells displaying power conversion efficiencies between 2.79% to 3.27%.

The primary disadvantage with dipcoating is the large observed variance in smoothness and uniformity of the conducting polymer coating. Often, rough, textured coatings resulting from incomplete wetting and/or agglomerated conjugated polymer chains are obtained. For instance, scanning electron micrographs (SEMs) of Sonkusale and Khademhosseini's aforementioned PANI-coated cotton threads reveal that the PANI coat is non-uniformly bulbous, microporous and rough on the micron length scale (Fig. 1c). In the long term, these bulbous regions are undesirable as they can potentially serve as points of de-adhesion and exfoliation during subsequent textile processing and body-mounting. Along the same lines, Gaudiana *et al.* explain in their report that diamond tip-extruded stainless steel thread needed to be used as the substrate onto which a solar cell was elaborated because these specialty threads displayed a particularly smooth, protrusion-free surface that allowed for smooth active layer coatings, which, in turn, lead to solar cells with functional rectification ratios. The presence of even a small number of rough surface features or active layer agglomerates on the fiber surface would lead to insurmountable shunting pathways that can significantly deteriorate device performance, even to the point of rendering it unfunctional.

Despite a large variation in observed coating morphology, dipcoating remains the most popular method of fiber/fabric functionalization to date. This is due, in part, to a selected number of conducting polymer formulations that yield smooth, functional coatings or composites with various natural and synthetic fibers and fabrics.

Fibers and fabrics dipcoated with aqueous solutions of PEDOT:PSS are the most common components of electronic textiles. Sotzing *et al.* created highly conductive fabrics by soaking a selection of fabrics in a commercially-available

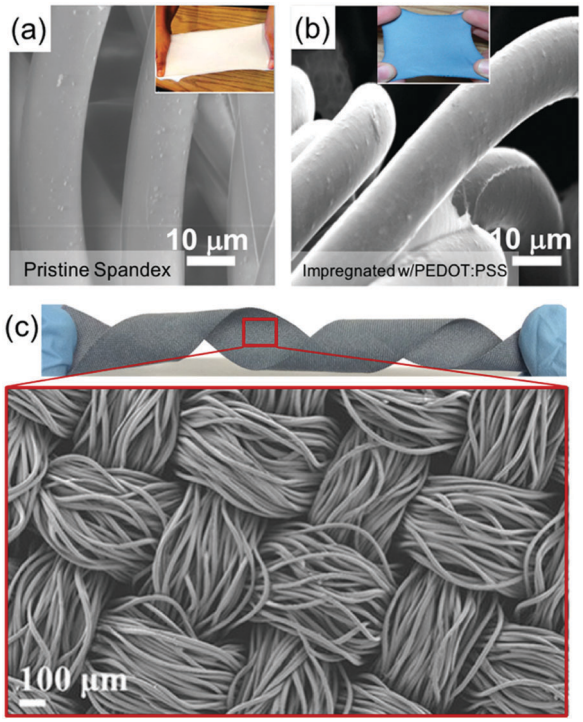

Fig. 2 (a) SEM of Spandex fabric used by Sotzing *et al.* The inset shows a photograph of this fabric. (b) SEM of Spandex dipcoated with PEDOT:PSS. The inset shows a photograph of this fabric. Adapted from ref. 11. (c) Photograph (top) and SEM (bottom) of a PEDOT:PSS coated polyester fabric reported by Lin *et al.* Adapted from ref. 18.

aqueous solution of PEDOT:PSS.[11] Fabrics investigated included: Spandex (50% nylon/50% polyurethane); cotton; polyester, 60% cotton/40% polyester; 95% cotton/5% lycra; 60% polyester/40% rayon; and 80% nylon/20% spandex. The conductive spandex fabric thus obtained (see Fig. 2b) had an average conductivity of 0.1 S cm^{-1} (for reference, the conductivity of a 100 nm-thick "conductive-grade" PEDOT:PSS film on glass is 1 S cm^{-1}). Subjecting the fabric to more than one soaking step increased its conductivity up to *ca.* 2.0 S cm^{-1} by increasing the weight fraction of the conducting polymer component.

It must be noted that fibers and fabrics can be swelled, *i.e.*, impregnated, by the electronically-active materials during dipcoating, depending on the soaking time and solvent used. Such swelling and impregnation events can change the mechanical properties of the starting fiber/fabric. Different fibers and fabrics display different degrees of uptake of various soaking solvents and conjugated polymers, approximately obeying a "like swells like" pattern of behavior. For instance, in the aforementioned work by Sotzing *et al.*, it was concluded that the PEDOT:PSS was not a continuous smooth film on a fabric surface but, rather, a homogeneously dispersed network of PEDOT:PSS nanoparticles impregnated within a fabric matrix, which formed a percolation pathway past a particular weight fraction (Fig. 2b). Further, the authors found that those fabrics with higher water uptake resulted in higher conductivities because they soaked up higher amounts of PEDOT:PSS from the aqueous dipcoating solution compared to more hydrophobic fabrics.[11]

The presence of various additives, both insulating polymer and small-molecule additives, in the dipcoating solution has been found to significantly affect the conductivities and/or sheet resistances of PEDOT:PSS coated fibers and fabrics by increasing the long-range order in the PEDOT domains of PEDOT:PSS. Changing the dipcoating solvent similarly affects sheet resistance and conductivity. Post-deposition treatments, such as thermal annealing and post-deposition exposure to small-molecule detergents or plasticizers vastly increases the observed conductivity of PEDOT:PSS coated fabrics. Mohanta *et al.* reported that the resistance of a PEDOT:PSS coated cotton yarn can be decreased from 2.32 MΩ cm^{-1} to 77 Ω cm^{-1} if the cotton yarn is first dipcoated in DMSO instead of water then washed with ethylene glycol before drying.[12] Similarly, Yun *et al.* reported that cotton and polyurethane fabrics dipcoated with PEDOT:PSS solutions containing a sodium dodecylsulfate (SDS) detergent displayed sheet resistances of 24 and 48 Ω sq^{-1}, respectively, with the cotton fabrics displaying lower sheet resistances because of a higher amount of impregnated PEDOT:PSS in these fabrics. Using these fabrics, the authors then created metal-free textile heaters by taking advantage of efficient Joule heating in these conductive fabrics.[13]

Hu *et al.* dipcoated both cotton and polyester yarns in an aqueous solution containing a mixture of PEDOT:PSS, multi-walled carbon nanotubes (MWCNTs) and a polyurethane binder in various ratios to create fabrics displaying thermoelectric properties.[14] In this report, the polyurethane functions as an insulating, hydrophobic polymer matrix that binds together the two conductive components (PEDOT:PSS and MWCNTs) in the dried coating. Synthetic polyester yarns were completely coated after five dipping-drying cycles. However, cotton yarns, which are more geometrically unorganized, remained non-uniformly coated, even after five dipping cycles. Accordingly, the non-uniformly coated cotton yarn displayed a resistance of 200 Ω cm^{-1}, whereas the uniformly-coated polyester yarns displayed a lower resistance of 50 Ω cm^{-1}.

Åkerfeldt *et al.* created conductive synthetic fabrics by dipcoating poly(ethylene terephthalate) (PET) fabrics into a mixture of aqueous PEDOT:PSS, Performax (a commercially-available aqueous solution of polyurethane and hydroxyethylcellulose that acted as a binder), ethylene glycol (a small-molecule surfactant), and an ethoxylated urethane (a rheology modifier).[15] Similar to previous reports, PEDOT:PSS was observed to impregnate into the PET substrates to produce conductive fabrics with smooth surfaces (Fig. 3). Dipcoating solutions containing the highest weight percent of the PEDOT:PSS component were, unsurprisingly, found to yield the most conductive fabrics after dipcoating/drying: sheet resistances as low as 12.7 Ω sq^{-1} were observed. Slow drying and post-deposition thermal annealing were also found to contribute to the low observed sheet resistance of these conductive fabrics. This work is notable because the authors perform extensive and systematic mechanical and abrasion testing on their conductive fabrics. A high PEDOT:PSS weight fraction (80 wt%) and the presence of an ethylene glycol surfactant in the dipcoating solution was found to produce conductive textiles with high tear strength.

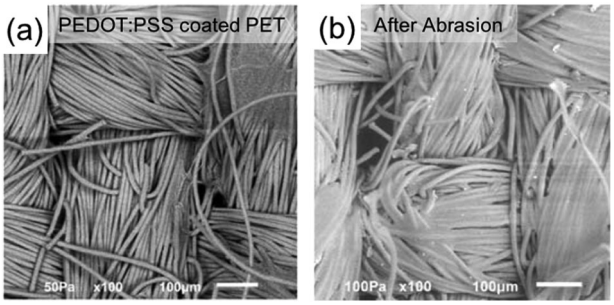

Fig. 3 (a) SEM of the most-conductive PEDOT:PSS coated fabric reported by Åkerfeldt *et al.* This sample had a sheet resistance of 12.7 Ω sq^{-1}. (b) SEM of this fabric after surface abrasion, revealing smearing of the conductive coating. Adapted from ref. 15.

However, these same samples demonstrated the greatest degree of coating degradation with abrasion (it was even visually apparent that the coatings were smeared and faded after abrasion, see Fig. 3b). Increasing the weight fraction of the polyurethane binder to 28% in the dipcoating solution afforded admirably abrasion-resistant coatings; however, an increased binder concentration also increased the sample's sheet resistance to 78.3 Ω sq^{-1}.[15]

Müller *et al.* used a dipcoating solution containing PEDOT:PSS, Zonyl FS-300 (binder), and either DMSO or ethylene glycol (surfactant) to impregnate/coat silk and cotton yarns.[16] The notable component here is the Zonyl FS-300 binder, which is a commercially-available fluoroalkyl-containing oligo(ethylene glycol) surfactant. After two dipcoating-drying-thermal annealing cycles, silk yarns with conductivities between 14 and 15 S cm^{-1} were obtained. Notably, these conductive yarns were found to be resistant to mechanical stress and laundering. The PEDOT:PSS dyed silk yarns maintained their bulk electrical conductivity after being subjected to repeated bending stresses and mechanical wear during sewing. No change in conductivity could be detected after four washing cycles in a household washing machine; however, the conductivity of the yarns decreased by a factor of 2 after five dry cleaning cycles.[16] Such varying responses to different laundering actions can be easily correlated to the Zonyl FS-300 binder: fluoroalkyl chains do not interact with the long alkyl chains of the surfactants found in most household laundry detergents (such as SDS) but are easily solvated by the halogenated solvents used in dry cleaning. Therefore, dry cleaning likely dissolves away some of the conductive coating, leading to higher observed resistances.

A few patterns can be gleaned from a survey of the literature reports highlighted thus far. First, certain conjugated polymers and their composites afford smooth coatings compared to others. In particular, PEDOT:PSS likely swells and impregnates most hydrophilic fibers, as opposed to forming a strictly surface coating, leading to highly-conductive fibers and fabrics due to high polymer loading. In contrast, poly(aniline) accumulates primarily on the surface of most fibers, which leads to rough, textured surfaces and low polymer loadings in the final fiber/fabric composite. Second, when using polymers that do not impregnate fibers/fabrics, threads/fibers with longer and monodisperse staple lengths, such as nylon, silk and synthetic threads, display smoother surface coatings in comparison to threads/fibers with short and/or polydisperse staple lengths, such as cotton threads and yarns. Third, the wash and wear resistance of conducting coatings obtained *via* dipcoating is controlled by the presence of carefully-chosen binders and/or surfactants in the dipcoating solution.

2.2 Devices

In addition to the few cases highlighted above, many other types of electronic devices are enabled by conductive fibers and textiles created using dipcoating. Ishida *et al.* constructed a single-type (*p*-type only) thermoelectric generator using square patches of a PEDOT:PSS coated cotton fabric sewn together with nickel foil, which yielded a thermoelectric power density of 4.5 μW cm^{-2} mg^{-1}.[17] Lin *et al.* fabricated thermoelectric fabrics by dipcoating prewoven polyester fabrics with PEDOT:PSS dispersed in DMSO.[18] The coating process was repeated twice to afford fabrics with a smooth surface (Fig. 2c), conductivities of 1.5 S cm^{-1} and a maximum power factor of 0.045 μW m^{-1} K^{-2} at 390 K. Single-type fabric thermoelectric generators were then created by stitching strips of this conductive fabric onto a raw polyester fabric backing and electrically connecting these strips with silver-coated nylon thread.

Inganäs *et al.* demonstrated that a conductive silk fiber could be utilized as the source–drain channel in an organic electrochemical transistor (OECT) by dipcoating either natural or recombinant silk fibers with poly(2,3-dihydrothieno[3,4-*b*]-[1,4]dioxin-2-yl-methoxy)-1-butanesulfonic acid (PEDOT:S). These dipcoated fibers exhibited conductivities as high as 0.044 S cm^{-1}.[19,20] In a different report, Inganäs *et al.* demonstrated a novel fiber-based OECT device architecture comprised of two PEDOT:PSS coated cotton yarns arranged in a cross geometry. One yarn comprised the source–drain channel and the second yarn acted as a gate electrode. A droplet of a polymer gel electrolyte placed at the intersection between the two yarns completed the gate–source conduction pathway.[21] Coppedè *et al.* also created several fiber-based OECTs using a PEDOT:PSS coated cotton yarn sewn onto an insulating substrate. Notably, human sweat was needed to complete a conductive channel between the gate and source electrodes in this device, allowing these OECTs to function as skin-mountable sensors to monitor the concentrations of varying analytes in human sweat.[22,23]

Andrew *et al.* used dipcoating to create all-textile triboelectric generators that generated power due to the creation of surface charge upon the physical contact of two fabric surfaces of opposite polarity (Fig. 4).[24] Cotton fabrics were dipcoated with a fluoroalkyl alkoxysiloxane compound, which formed a rugged, polymeric fluoroalkylsiloxane surface coating on the cotton fabrics upon drying. This dipcoated cotton fabric was then sewn onto a conductive fabric electrode and subsequently placed atop a complementary electrode (comprised of a nylon fabric sewn onto a conductive fabric) to create an all-textile triboelectric generator. This device yielded an average power output of 13 μW cm^{-2} when the stacked electrodes were connected to a 50 MΩ load and lightly patted together.

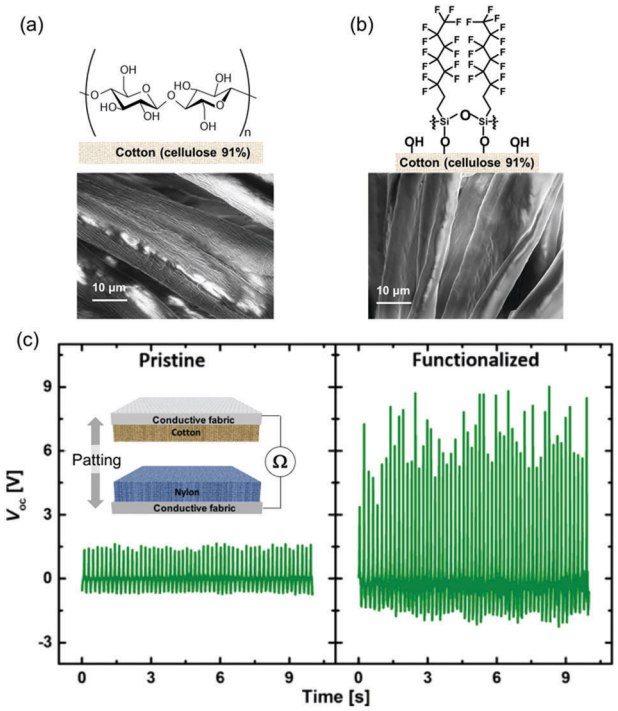

Fig. 4 (a) SEM of pristine cotton fabric. (b) SEM of cotton cloth dipcoated with a fluoroalkylsiloxane. (c) Voltage outputs obtained upon light patting of two textile triboelectric generators constructed using either pristine cotton cloth (left) or fluoroalkylsiloxane coated cotton cloth (right). A cartoon of the device is provided as an inset. Adapted from ref. 24.

This work is interesting because the densely microstructured surface of cotton textiles was integral in creating useable surface charge density upon physical contact (typically, planar surfaces do not produce notable triboelectric power).

3. Vapor coating

Vapor phase polymerization of conducting polymers is a nascent technique that combines polymer synthesis and deposition into one step.[25–27] This method allows for a conjugated polymer coating to be directly formed on any textile or fiber substrate in the vapor phase, without the need for detergents, fixing agents or surface pretreatments, which can reduce the overall number of steps involved in current textile manufacturing routines and curtail the significant solvent use associated with textile production. Vapor deposition is an attractive technique that allows for uniform and conformal coating[28] of arbitrary substrates of any surface topography/roughness and produces conductive materials without any insulating moieties. Vapor deposited coatings are often thin enough such that the original mechanical properties of the substrate (and not that of the coating) will be the dominant observable.[29]

Two main components are required for vapor deposition: a conjugated monomer and oxidant. Monomers include 3,4-ethylenedioxythiophene (EDOT), aniline (ANI) and pyrrole (Py). A variety of iron(III) salts are used as the oxidant, including iron(III) chloride and iron(III) *p*-toluenesulfonate. Two major subclasses of vapor deposition methods exist, both of which have been used to coat textiles and yarns with conducting polymers. The first technique is called vapor phase polymerization (VPP) and involves impregnating the iron oxidant into a fiber/fabric *via* dipcoating or dropcasting and then exposing this iron-impregnated fiber/fabric to vapors of the desired monomer in a closed chamber. The second vapor deposition technique is called oxidative chemical vapor deposition (oCVD) and is distinct from VPP in that both the oxidant and monomer are introduced simultaneously in the vapor phase to create a conjugated polymer film. oCVD is typically conducted in a reactive vapor deposition chamber, although the requirements for this chamber are not exact, and a variety of widely-available reaction glassware can be adapted to effect polymer deposition. The basic requirements for a deposition chamber include a controlled inlet for the gaseous monomer, a heated crucible to generate oxidant vapor, a heated surface to hold the fabric/fiber substrate in the vicinity of the oxidant vapor plume, and a vacuum pump. Fig. 5a shows the setup of an oCVD chamber used by Andrew *et al.*[30]

In both vapor deposition methods, the gaseous monomer reacts with an oxidant at or near a heated substrate to form oligomers and polymers that will be deposited onto the substrate (Fig. 5b).[31] Exposed oxidants on the surface of the fiber/fabric create reactive radical cations of the monomer at or near the surface of the substrate, which then react with other monomers to produce a growing polymer chain. Depending on the chemical composition of the fiber/fabric substrate, the monomer radical cations can also react with functional groups on the fiber/fabric surface to afford mechanically-stable surface-grafted conjugated polymer films on fibers/fabrics. Notably, whereas the degradation and swelling of a fiber/fabric in certain solvents needs to be considered when using solution-based polymerization and/or deposition methods, this is not a concern with vapor deposition methods.[32]

All vapor deposition procedures are followed by necessary rinsing steps to remove residual oxidant and other small-molecule reaction byproducts from the deposited polymer film. Therefore, this coating process is not entirely solvent-free, though its overall solvent footprint is smaller compared to other solution-phase coating approaches. Rinsing in methanol or sulfuric acid/methanol mixtures effectively removes residual iron salts from the films[30] and also improves the conductivity of the isolated conjugated polymer films. PEDOT films on glass displaying conductivities as high as 2500 S cm^{-1} and 1500 S cm^{-1} have been obtained *via* VPP and oCVD, respectively.[33]

Dall'Acqua and Tonin *et al.* created poly(pyrrole) (PPy) coated cellulose textiles using VPP for eventual use as an electroactive membrane in fuel cells. Fabrics were first soaked in ferric chloride hexahydrate and then exposed to vaporized pyrrole to afford PPy coatings. Coating uniformity was affected by the weight loading and degree of impregnation of the iron oxidant—higher oxidant loadings lead to greater oxidant impregnation in the cellulose textiles, which, in turn, yielded smoother and more-uniform PPy coatings upon exposure to

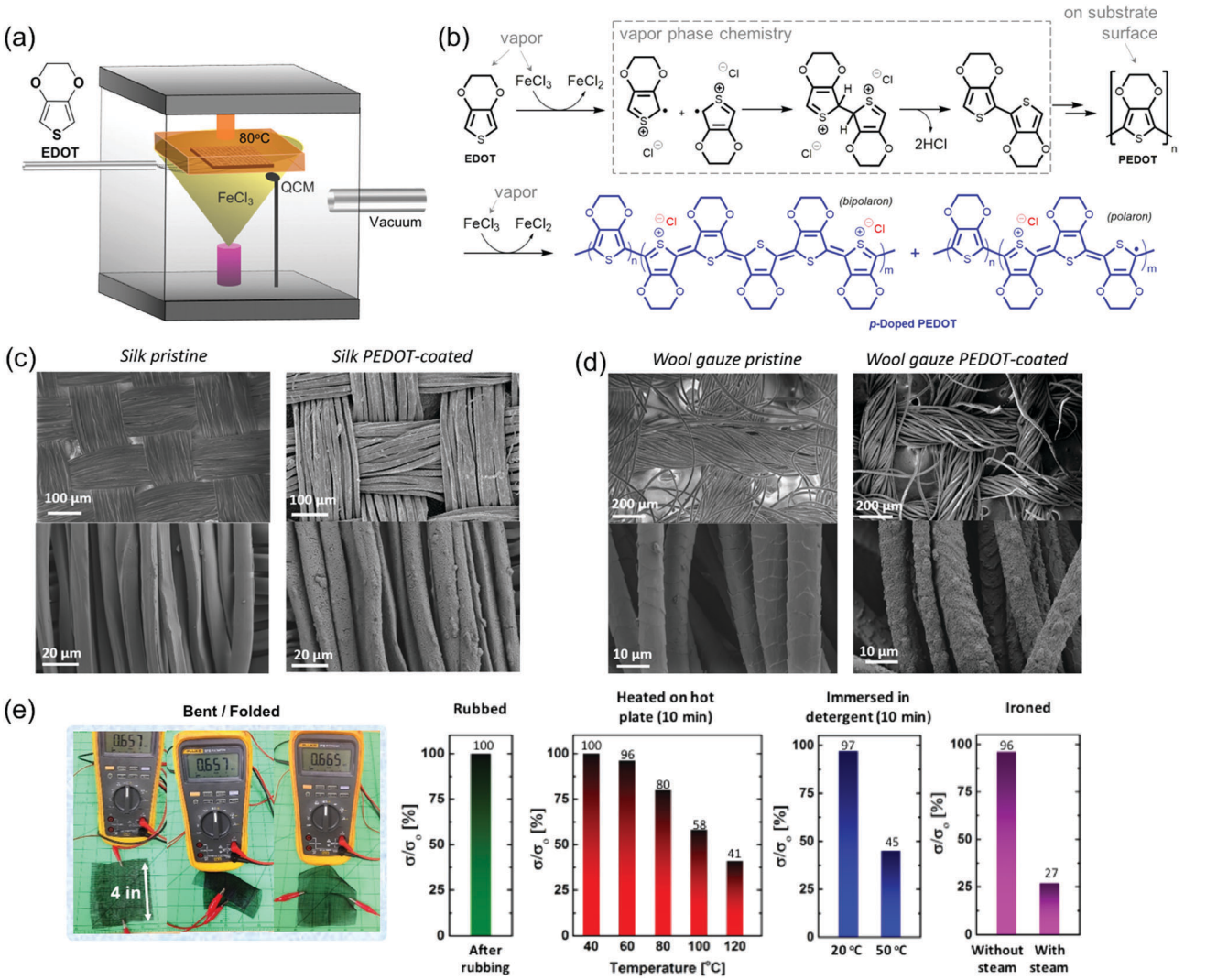

Fig. 5 (a) Schematic of a chamber used to perform oxidative chemical vapor deposition (oCVD). (b) Operative vapor polymerization reaction during the oxidative chemical vapor deposition of PEDOT. (c) SEMs of silk fabrics before and after coating with PEDOT *via* oCVD. (d) SEMs of wool gauze before and after coating with PEDOT *via* oCVD. (e) Mechanical and chemical stability of a 4 × 4 inch conductive PEDOT-coated pineapple fiber fabric to various applied stresses. Adapted from ref. 30.

pyrrole vapor.[34] Shang *et al.* investigated the influence of reaction conditions, such as oxidant loading, reaction time and reaction temperature, on the structure and electronic properties of PPy coatings created on PET fabrics using VPP. The authors concluded that oxidant loading did not have a notable effect on the conductivity of the PPy coating obtained by VPP and that intermediate reaction times (4–5 hours) at low temperatures (4 oC) afforded the smoothest, most uniform PPy coating with the lowest sheet resistance (250 Ω sq^{-1}).[35]

Skrifvars *et al.* used VPP to deposit PEDOT onto textiles.[36] Contrary to observations made for dipcoated samples, the authors determined that pre-treating textiles with organic solvents reduced the electrical conductivity of PEDOT coatings obtained *via* VPP. Further, brittle, flaky PEDOT coatings were obtained on solvent-treated textiles. Different types of oxidants were explored for the VPP of PEDOT. PEDOT coatings obtained using $FeCl_3$ as the oxidant displayed high electrical conductivity, whereas samples obtained using iron(III) *p*-toluenesulfonate as the oxidant resulted in strong mechanical properties. Non-natural, designer fibers have also been used as substrates for VPP. Laforgue *et al.* exposed electrospun fiber mats comprised of the oxidant, iron(III) *p*-toluenesulfonate, dispersed in an insulating polymer matrix to EDOT vapor in order to create quasi-pure PEDOT nanofibers with a measured electrical conductivity of 60 S cm^{-1}.[37]

Bashir and Skrifvars *et al.* used oCVD to deposit PEDOT onto polyester yarns, obtaining products with conductivities of 14.2 S cm^{-1}.[38] Andrew *et al.* used oCVD to transform familiar, off-the-shelf, plane-woven fabrics, such as linen, silk and bast fiber fabrics, into metal-free conducting electrodes (Fig. 5c and d).[30] Four square inch swatches of pineapple fiber fabric coated with only a 500 nm thick PEDOT surface coating displayed a sheet resistance of 300 Ω sq^{-1} and conductivities of 298 S cm^{-1}. For reference, 18 µm thick films of commerically-available

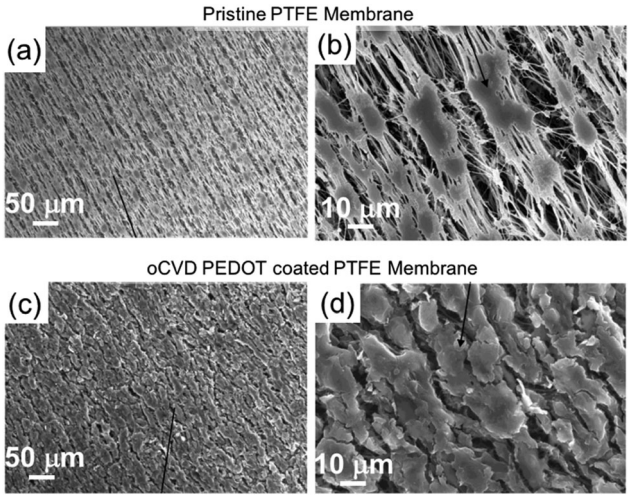

Fig. 6 (a and b) SEMs of a porous PTFE membrane at two different magnifications. (c and d) SEM of these membranes after PEDOT coating using oCVD. Adapted from ref. 39.

"high conductivity grade" PEDOT:PSS on glass display sheet resistances of 500 Ω sq^{-1} and conductivities of 200 S cm^{-1}. These naked fabric electrodes were resistant to mechanical abrasion and were stable after laundering, solvent washing (organic, halogenated and aqueous solvents) and ironing, despite the absence of a protective binder or other such cladding. The electrical properties of these fabric electrodes were also found to be stable to bending/folding, rubbing, body heat, cold laundering, dry cleaning and dry ironing (Fig. 5e).

Vapor deposition methods afford highly conformal conjugated polymer coatings that preserve the topography and texture of the underlying substrate with high fidelity. This feature can be advantageous when working with certain morphologically-distinct substrates. Bashir *et al.* proved this point by coating porous poly(tetrafluoroethylene) (PTFE) membranes with PEDOT *via* oCVD and demonstrating that the vapor deposited PEDOT coating did not clog the membrane pores.[39] Fig. 6 shows the PTFE membrane pores before and after coating with PEDOT. Additionally, the necessary post-deposition sulfuric acid rinse to remove residual iron oxidant was also found to lower the sheet resistance of the PEDOT-coated membranes to a final value of 0.8 kΩ after 72 hours.

As summarized in Fig. 7, Andrew *et al.* also reported a unique feature that arises when prewoven textiles are coated using oCVD: since the polymer coating is conformal and since each face of a fabric can be selectively coated in a reactive vapor deposition chamber (unlike dipcoated fabrics), the warp and weft threads of a plain-woven fabric act as each others' shadow masks at each weave intersection. This ultimately means that the continuity of the conducting polymer coating on each warp and weft thread of a plain-woven fabric is determined by the number of weave intersections in the fabric, which, in turn, means that the effective conduction length of the conductive coating is dependent on weave density. Variations of up to three orders of magnitude were observed for PEDOT-coated cotton fabrics of differing weave density (Fig. 7c), despite being

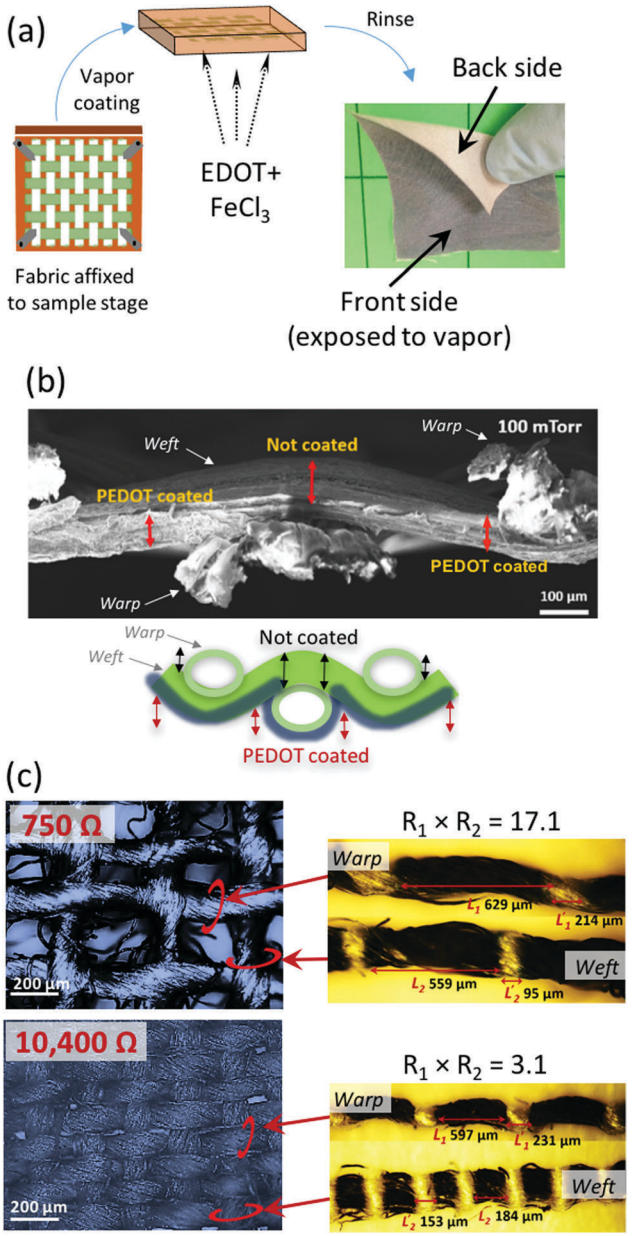

Fig. 7 (a) Illustration of the substrate holder in an oCVD chamber and photograph of a 4 × 4 inch silk fabric after PEDOT coating *via* oCVD revealing two distinct faces (coated face and uncoated face). (b) Cross-section SEM of a silk fabric coated with PEDOT *via* oCVD showing coated and uncoated regions. (c) Optical micrographs of two PEDOT-coated cotton cloths with differing weave densities (left) and of a warp/weft yarn pulled out from these cloths after PEDOT deposition *via* oCVD (right). The micrographs of the warp/weft yarns reveal that the PEDOT film on each yarn is discontinuous due to self-shadowmasking during oCVD. Adapted from ref. 30.

comprised of the same thread and being coated simultaneously. Counterintuitively, airy, open-weave fabrics display the highest conductivities (despite their reduced surface area) because they contain fewer weave intersections and, therefore, the most continuous PEDOT coatings.[30]

Textile scientists have traditionally shied away from using vapor deposition methods to create various textile-based

electronics because of the perceived difficulty and high cost of scaling up vapor coating chambers to satisfy the high volume demand of the textile industry. However, as described by Gleason *et al.*, advancements made over the past decade have resulted in the use of vapor deposition methods to stain-guard carpets, lubricate large area mechanical components and protect microelectronic devices, demonstrating that vapor coating methods are indeed conducive to large-scale, high-throughput manufacturability.[40] Moreover, the tremendous wash and wear resistance of vapor deposited films is an intrinsic property, as opposed to a feature imparted by the addition of a carefully-chosen binder, as in the case of conductive fibers/fabrics created *via* dipcoating. The electrical properties of the conjugated polymer films created by vapor deposition are also superior to those created from commercial conducting polymer inks: vapor-deposited conducting polymer films lack an insulating component (such as PSS or solubilizing side chains on each repeat unit) and can therefore support much higher current densities per unit volume than their solution-processed counterparts.

4. Electrochemical coating

Electrochemical polymerization is another coating method that combines polymer synthesis and deposition into one step. A monomer is dissolved in an appropriate solvent along with an electrolyte salt and a linearly varying (triangle-wave) potential is applied using a voltage source and, typically, a three-electrode setup (working, counter and reference electrodes). Monomer oxidation occurs when sufficient positive bias is applied, which initiates polymerization at the working electrode.[41] Several textiles have been coated with conducting polymers *via* electropolymerization.[42]

The main requirement for electrochemical deposition of conjugated polymers is a conductive working electrode. Since standard fiber or fabric substrates are normally insulating, they cannot be directly used as an electrode onto which a polymer coating is deposited *via* electrochemical means. One creative approach for depositing polymers onto an insulating fiber substrate is to simply wrap a metal working electrode with the fiber, allowing the polymers formed in the vicinity of the working electrode to passively coat the fiber. Gupta *et al.* coated natural fibers, such as silk, cotton, and wool, with poly(pyrrole) in this fashion, using a platinum wire working electrode.[43]

Most reports that use electrochemical polymerization to form conjugated polymer coatings first create a thin conductive base coat, or seed layer, on the fiber/fabric using dipcoating, VPP or solution polymerization, which then allows the fiber/fabric to directly act as the working electrode. In this sense, electrochemical polymerization can be best considered as a method with which to increase the thickness of a conductive coating on fibers/fabrics. Under optimized conditions, the morphology of the electrodeposited polymer coating is largely determined by the morphology of the underlying seed layer.

Cases *et al.* used this approach to make conductive polyester textiles. Textiles were first coated with a seed layer of poly(pyrrole) *via in situ* solution polymerization (see Section 4), and this coated textile was subsequently used as the working electrode for an electrochemical polymerization of pyrrole or aniline. The conductivities of the resulting textiles were approximately 20 $\Omega\ sq^{-1}$ for both poly(pyrrole) and poly(aniline) coated textiles.[44,45] Murphy *et al.* also prepared poly(pyrrole)-coated textiles using this technique, however the textile substrate was silk instead of polyester. The authors demonstrated that these poly(pyrrole) coated conducting silks are uniquely-biocompatible biosensors.[46] Similarly, Jager *et al.* created metal-free textile actuators that act as artificial muscles using poly(pyrrole)-coated conductive yarns obtained *via* electrochemical polymerization.[47] Single- and two-ply twisted Lyocell cellulose staple yarns were first coated with a seed layer of PEDOT using vapor phase polymerization (see Section 2). Next, these conductive yarns were used as the working electrode to effect electrochemical polymerization of poly(pyrrole). These textile actuators showed a 27% decrease in actuation force when cycled between −1 and 0.5 V at 0.05 Hz for 8000 cycles. Notably, uniform polymer coatings were found to be integral to enabling macroscale actuation and the observed uniformity of the PPy coat was mostly ascribed the use of vapor phase polymerization to create a smooth PEDOT seed layer. Krishnamoorthy *et al.* transformed various naturally-occurring fibers/threads into fiber supercapacitors using, first, a novel redox reaction to deposit a gold coating onto these natural fibers and subsequently creating a PEDOT layer on the gold-coated fibers using electrochemical polymerization. These gold/PEDOT coated fibers displayed capacitances as high as 254 $F\ g^{-1}$.[48]

The morphology of electrodeposited conjugated polymer films on fibers/fabrics is also influenced by the rate at which the applied potential is varied (*i.e.*, the scan rate). Cases *et al.* investigated scan rate effects on the morphology of poly(aniline) films deposited onto polyester fabrics *via* electrochemical polymerization.[49] Notably, the poly(aniline) coatings displayed "centipede-like" features—*i.e.*, two rows of fuzzy polymer nanofibers branching from a common core—at low scan rates (Fig. 8), which is a highly-unusual and unmatched solid-state structure. The surface resistivity of the poly(aniline) coated fabrics was as low as 3 $\Omega\ sq^{-1}$ for samples synthesized at a scan rate of 1 $mV\ s^{-1}$.

5. *In situ* solution polymerization

Certain conducting polymers are not readily available as stable, pre-formulated conducting inks—for example, poly(pyrrole) (PPy) and poly(aniline) (PANI). In these cases, the polymer can be chemically synthesized in the presence of a desired substrate to simultaneously effect polymerization and deposition. We label this method as *in situ* solution polymerization. In this method, a substrate is placed into a solution containing the desired monomer and, if appropriate, other reagents, after which an oxidant is added to solution to initiate polymerization. A certain fraction of the polymers formed in the reaction solution will passively adhere to the surface of the substrate. Depending the surface chemistry of the

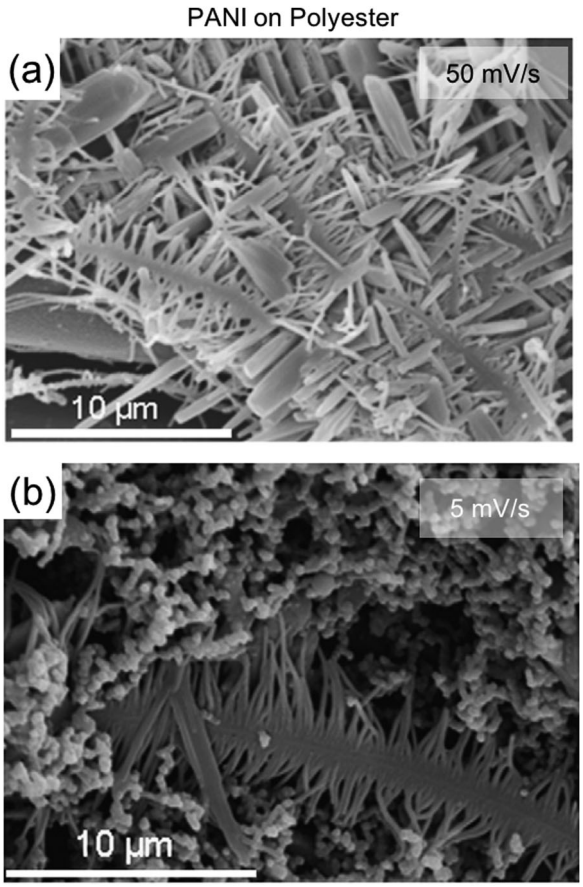

Fig. 8 SEMs of poly(aniline) films deposited on conductive polyester fabrics *via* electrodeposition at a scan rate of (a) 50 mV s^{-1} or (b) 5 mV s^{-1}. Adapted from ref. 49.

substrate and the presence/absence of reactive functional groups, reactive monomers or growing polymer chains can also become covalently attached to the substrate during the reaction.

Though seemingly straight-forward, *in situ* solution polymerization is hard to control in real time. Ways to control mass transport during polymerization/deposition are minimal and strategies to direct film growth kinetics are hard to enforce. The conjugated polymer coatings obtained *via in situ* solution polymerization display the highest degree of nonuniformity, surface roughness and batch-to-batch variance among all the fabrication methods summarized in this article (Fig. 9). Small changes in reaction conditions (such as stirring/no stirring), monomer/oxidant concentrations and reagent addition order can lead to significant differences in film crystallinity/morphology, coating uniformity and correlated electronic properties. Moreover, some fabrics have been observed to degrade under the acidic reaction conditions necessary to effect pyrrole and aniline polymerization in solution. Therefore, this technique is best used with caution.

Kang *et al.* explored various *in situ* solution polymerization procedures to create PEDOT-coated nylon, PET and PTT fabrics, with the aim of optimizing their conductivities.[50] The authors found that most solution polymerization conditions degraded and/or partially dissolved nylon fibers, leading to products with

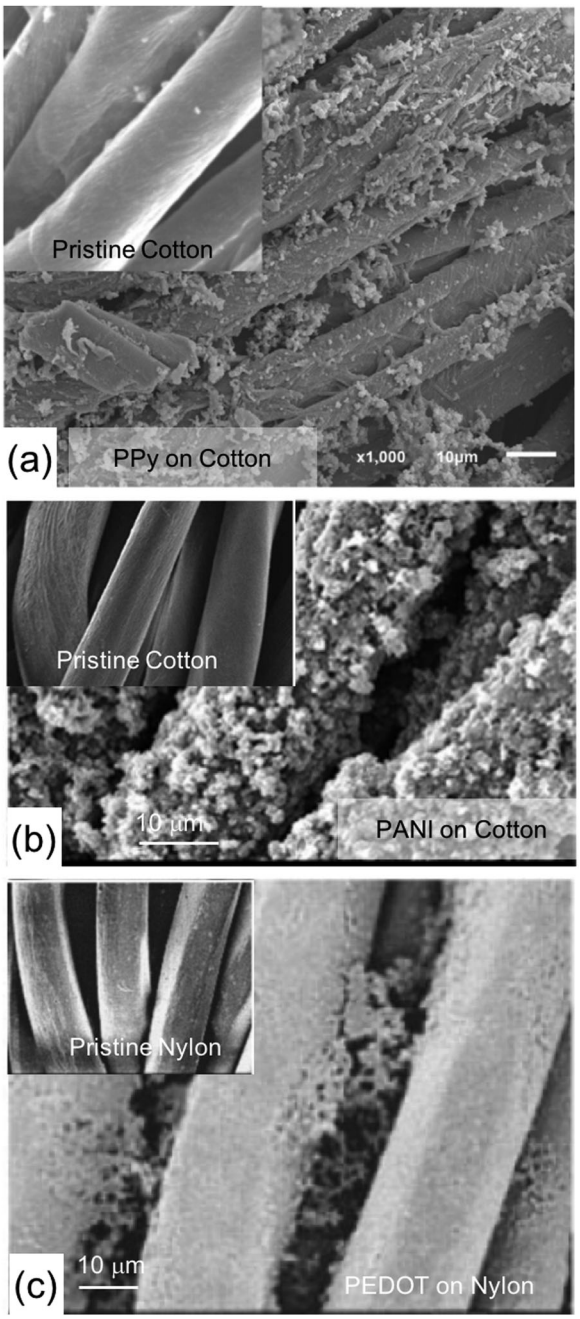

Fig. 9 SEMs of conducting polymer films on fabrics deposited *via in situ* solution polymerization. (a) Poly(pyrrole) on cotton. Adapted from ref. 52. (b) Poly(aniline) on cotton. Adapted from ref. 53. (c) PEDOT on nylon showing nylon degradation. Adapted from ref. 50.

inferior mechanical properties. Varesano *et al.* created conductive PPy-cotton fabrics with sheet resistances as low as 2.18 Ω sq^{-1}.[51] Xu and Xu *et al.* also used *in situ* solution polymerization to create PPy-coated cotton fabrics that served as supercapacitors with a specific capacitance of up to 325 F g^{-1} and energy densities up to 24.7 W h kg^{-1}.[52] Akşit *et al.* coated cotton fibers with PANI and subsequently doped these films with barium ferrite, achieving sheet resistances as low as 350 Ω cm^{-1}.[53] Stejskal *et al.* used the reducing ability of PPy and PANI coatings on cotton fabrics to

deposit silver nanoparticles from silver nitrate solutions onto the surface of the fabrics. These silver/PANI and silver/PPy coated cotton fabrics displayed notable antimicrobial activity and cytotoxicity.[54]

Currently, *in situ* solution polymerization has primary utility in creating conducting polymer-coated electrospun fibers and mats.[55] Jiang and Hou *et al.* created high-performance lithium-ion battery separator membranes by coating electrospun polyimide nanofibers with PANI using *in situ* solution polymerization.[56] Mo *et al.* coated nanofibrous membranes created by co-electrospinning poly(L-lactic acid-*co*-ε-caprolactone) and silk fibroin with PPy.[57] These conductive and biocompatible membranes were used for nerve tissue repair and regeneration.

6. Miscellaneous coating methods

Due to the popularity and utility of PEDOT:PSS coated textiles, there exist isolated reports in which creative or unusual fabrication methods are used to access electronically-active textiles. One such example comes from Kim *et al.* who used blade coating to coat PEDOT:PSS onto the surface of a specially-extruded synthetic fabric comprised of polyester/silver nanowires/graphene.[58] The bladecoated PEDOT:PSS film served as a hole-transport/electron-blocking layer for a semiconducting polymer-fullerene bulk heterojunction solar cell that was subsequently elaborated onto the fabric surface. The solar textile thus obtained demonstrated a power conversion efficiency of 2.27% and a specific power of 0.45 W g^{-1}.

Sotzing *et al.* created patterned circuits on the surface of PET fabrics by inkjet printing a specially formulated PEDOT:PSS ink containing commercially-available "high conductivity grade" PEDOT:PSS, ethanol, and diethylene glycol.[59] The ratios of these three components were optimized to obtain an appropriate ink viscosity. The sheet resistance of these inkjet printed wires was high (3185.7 Ω sq^{-1}), which the authors ascribed to a low concentration of PEDOT:PSS in the deposited film: a 125 mm^2 area was found to contain only 0.15 mg of PEDOT:PSS, even after 10 printing passes. The authors then created patterned circuit pathways on the surface of PET fabrics using a stenciling method.[56] A plastic stencil was fashioned and placed atop the PET fabric, after which a concentrated PEDOT:PSS solution was stippled onto the PET fabric through the stencil using a sponge. The sheet resistance of the wires thus fabricated was 2.7 Ω sq^{-1}, which was attributed to an increased amount of deposited PEDOT:PSS: the sponge stencil method deposited 1.59 mg of PEDOT:PSS over a 125 mm^2 area. The current carrying capacity (CCC) for these PEDOT:PSS wires were measured and compared against silver-coated conductive fabrics and carbon nanotube-impregnated paper (buckypaper). The CCC of the PEDOT:PSS circuit on PET fabrics was measured to be 1000 A cm^{-2}, comparable to that of buckypaper but lower than that of silver-coated bamboo cloths.

7. Conclusions and outlook

Commonly-available, mass-produced fabrics, yarns and threads can be transformed into a plethora of wearable, skin-mountable and/or biocompatible electronic devices upon being coated with films of intrinsically conducting polymers, such as poly(aniline), poly(pyrrole), and poly(3,4-ethylenedioxythiophene). A variety of coating methods can be used to create conducting polymer coatings on traditional textile materials, including dipcoating, vapor deposition, electrochemical deposition, *in situ* solution polymerization, blade coating and inkjet printing.

Tremendous variation in the surface morphology of conjugated polymer-coated fibers can be observed with different coating or processing conditions. The morphology of the conjugated polymer active layer determines electrical performance and, most importantly, device ruggedness. The mechanical demand placed on fibers/fabrics during typical textile manufacturing processes, such as weaving, knitting and sewing, is uniquely high.[10] Further, any textile-based device will be subjected to significant strain, friction forces and chemical exfoliation during wear, laundering, and/or ironing. Therefore, for fiber- and fabric-based devices, in particular, the stability of a conductive coating against high friction forces, extreme bending radii and other large, cyclic mechanical stresses is paramount. To survive these stresses, electronically-active coatings must be smooth, uniform, conformal and, ideally but not necessarily, covalently-tethered to the surface of a fiber to limit exfoliation and de-adhesion events. In this article we highlight recent, notable approaches to coat familiar, mass-produced threads, yarns, or fabrics with electronically-active conjugated polymers to produce textile-based electronic devices, placing emphasis on the influence of the coating method on active layer morphology and device stability.

Dipcoating is, in essence, the same as the age-old practice of textile dyeing and, to date, remains the most prevalent and straight-forward method by which conductive fibers/fabrics are created. However, the conducting polymer inks that are necessary for this process are industrially-produced at much smaller scales than traditional textile dyes and are, therefore, far more expensive. Moreover, large variances in the smoothness and uniformity of the conducting polymer coatings obtained *via* dipcoating are known. Often, rough, textured coatings resulting from incomplete wetting and/or agglomerated conjugated polymer chains can be observed.

Another important consideration is the increasingly-pernicious issue of textile pollution. As reported in *Chem. Eng. News*,[60] the World Bank estimates that 20% of water pollution globally is caused by textile processing. Textile and garment production is water-intensive, consuming approximately 700 gallons of water to produce a T-shirt and 1800 gallons of water to produce a pair of jeans. Treating such large volumes of waste water is time- and energy-intensive, and expensive. Therefore, it behooves the academic community to concomitantly innovate safer, less-toxic chemicals and establish alternative approaches to process and dye textiles for nascent technological applications.

A young topic of academic research is the exploration of reactive vapor deposition methods to create electronically-active textiles. Vapor coating methods allow for a conjugated polymer to be directly formed on any textile or fiber substrate in

the vapor phase, without the need for detergents, fixing agents or surface pretreatments, which can reduce the overall number of steps involved in current textile manufacturing routines and curtail the significant solvent use associated with textile production. Further, vapor coating yields uniform and conformal films on fiber/fabric surfaces and produces conductive materials without any insulating moieties. Recent industrial endeavors have resulted in the use of vapor deposition methods to stain-guard carpets, lubricate large area mechanical components and protect microelectronic devices,[40] demonstrating that vapor coating methods can be feasibly incorporated into large-scale, high-throughput manufacturing routines. Nonetheless, various aspects still need optimization: new chamber designs[61] and coating stages are needed to process and coat large spools of thread; new, more efficient vapor phase polymerization chemistries are needed to decrease the duration of each coating cycle (typically 20 minutes) and allow for high-throughput textile production; and new chemistries are also needed to eliminate the use of heavy metal oxidants during the coating process.

A remarkable diversity of textile- or fiber-based electronic devices have been demonstrated thus far, including physiochemical sensors, thermoelectric fibers/fabrics, heated garments, artificial muscles and textile supercapacitors. Though their performance and longevity do not currently match those of analogous devices built on rigid substrates, such as glass and silicon, recently-reported fiber- and fabric-based devices demonstrate acceptable device metrics to warrant further elaboration. The major guiding principle for optimizing textile-based wearable technology, in particular, should be ruggedness and haptic perception, which can uniquely determine the difference between success (*i.e.*, widespread adoption) and failure, irrespective of device metrics. Especially for skin-mountable devices and smart garments, the intrinsic breathability and familiar feel of fabrics needs to be maintained, as these features cannot be replicated by devices built on plastic substrates, no matter how thin or flexible these devices can be made. In short, the challenge to device engineers in the near-term is to demonstrate that textile-based devices are truly "wearable," meaning that they retain the feel, weight, breathability and pliability of standard fabrics.

Acknowledgements

T. L. A. gratefully acknowledges financial support from the US Air Force Office of Scientific Research, under Agreement number FA9550-14-1-0128, and the David and Lucille Packard Foundation for graciously enabling parts of the exploratory research highlighted herein.

References

1 D.-H. Kim, N. Lu, R. Ma, Y.-S. Kim, R.-H. Kim, S. Wang, J. Wu, S. M. Won, H. Tao, A. Islam, K. J. Yu, T.-I. Kim, R. Chowdhury, M. Ying, L. Xu, M. Li, H.-J. Chung, H. Keum, M. McCormick, P. Liu, Y.-W. Zhang, F. G. Omenetto, Y. Huang, T. Coleman and J. A. Rogers, *Science*, 2011, **333**, 838–843.
2 P. Mostafalu, M. Akbari, K. A. Alberti, Q. Xu, A. Khademhosseini and S. R. Sonkusale, *Microsyst. Nanoeng.*, 2016, **2**, 16039.
3 G. Schwartz, B. C.-K. Tee, J. Mei, A. L. Appleton, D. H. Kim, H. Wang and Z. Bao, *Nat. Commun.*, 2013, **4**, 1859.
4 T. F. O'Connor, A. V. Zaretski, S. Savagatrup, A. D. Printz, C. D. Wilkes, M. I. Diaz, E. J. Sawyer and D. J. Lipomi, *Sol. Energy Mater. Sol. Cells*, 2016, **144**, 438–444.
5 K. Jost, G. Dion and Y. Gogotsi, *J. Mater. Chem. A*, 2014, **2**, 10776–10787.
6 (*a*) M. Kaltenbrunner, M. S. White, E. D. Glowacki, T. Sekitani, T. Someya, N. S. Sariciftci and S. Bauer, *Nat. Commun.*, 2012, **3**, 770; (*b*) M. Kaltenbrunner, T. Sekitani, J. Reeder, T. Yokota, K. Kuribara, T. Tokuhara, M. Drack, R. Schwodiauer, I. Graz, S. Bauer-Gogonea, S. Bauer and T. Someya, *Nature*, 2013, **499**, 458–463; (*c*) M. S. White, M. Kaltenbrunner, E. D. Glowacki, K. Gutnichenko, G. Kettlgruber, I. Graz, S. Aazou, C. Ulbricht, D. A. M. Egbe, M. C. Miron, Z. Major, M. Scharber, T. Sekitani, T. Someya, S. Bauer and N. S. Sariciftci, *Nat. Photonics*, 2013, **7**, 811–816; (*d*) M. Hamedi, R. Forchheimer and O. Inganas, *Nat. Mater.*, 2007, **6**, 357–362.
7 (*a*) Z. B. Yang, J. Deng, X. L. Chen, J. Ren and H. S. Peng, *Angew. Chem., Int. Ed.*, 2013, **52**, 13453–13457; (*b*) M. R. Lee, R. D. Eckert, K. Forberich, G. Dennler, C. J. Brabec and R. A. Gaudiana, *Science*, 2009, **324**, 232–235; (*c*) Z. B. Cai, L. Li, J. Ren, L. B. Qiu, H. J. Lin and H. S. Peng, *J. Mater. Chem. A*, 2013, **1**, 258–261; (*d*) L. X. Zheng, X. F. Zhang, Q. W. Li, S. B. Chikkannanavar, Y. Li, Y. H. Zhao, X. Z. Liao, Q. X. Jia, S. K. Doorn, D. E. Peterson and Y. T. Zhu, *Adv. Mater.*, 2007, **19**, 2567–2570; (*e*) Z. B. Yang, J. Deng, X. L. Chen, J. Ren and H. S. Peng, *Angew. Chem., Int. Ed.*, 2013, **52**, 13453–13457; (*f*) R. Ma, J. Lee, D. Choi, H. Moon and S. Baik, *Nano Lett.*, 2014, **14**, 1944–1951; (*g*) J. A. Lee, M. K. Shin, S. H. Kim, H. U. Cho, G. M. Spinks, G. G. Wallace, M. D. Lima, X. Lepro, M. E. Kozlov, R. H. Baughman and S. J. Kim, *Nat. Commun.*, 2013, **4**, 1970.
8 T. Chen, L. Qiu, Z. Yang and H. Peng, *Chem. Soc. Rev.*, 2013, **42**, 5031; M. Peng and D. Zou, *J. Mater. Chem. A*, 2015, **3**, 20435–20458.
9 (*a*) K. Jost, C. R. Perez, J. K. McDonough, V. Presser, M. Heon, G. Dion and Y. Gogotsi, *Energy Environ. Sci.*, 2011, **4**, 5060–5067; (*b*) L. B. Hu, M. Pasta, F. L. Mantia, L. F. Cui, S. Jeong, H. D. Deshazer, J. W. Choi, S. M. Han and Y. Cui, *Nano Lett.*, 2010, **10**, 708–714.
10 *Smart Textiles and Their Applications*, ed. V. Koncar, Woodhead Publishing, 2016.
11 Y. Ding, M. A. Invernale and G. A. Sotzing, *ACS Appl. Mater. Interfaces*, 2010, **2**, 1588–1593.
12 K. N. Amba Sankar and K. Mohanta, *AIP Conf. Proc.*, 2016, **1731**, 120019.
13 C. Yeon, G. Kim, J. W. Lim and S. J. Yun, *RSC Adv.*, 2017, **7**, 5888–5897.
14 Q. Wu and J. Hu, *Composites, Part B*, 2016, **107**, 59–66.
15 M. Åkerfeldt, M. Strååt and P. Walkenstrøm, *Text. Res. J.*, 2013, **83**, 2164–2176.
16 J. D. Ryan, D. A. Mengistie, R. Gabrielsson, A. Lund and C. Müller, *ACS Appl. Mater. Interfaces*, 2017, **9**, 9045–9050.
17 K. Kirihara, Q. Wei, M. Mukaida and T. Ishida, *Synth. Met.*, 2017, **225**, 41–48.
18 Y. Du, K. Cai, S. Chen, H. Wang, S. Z. Shen, R. Donelson and T. Lin, *Sci. Rep.*, 2015, **5**, 6411.
19 C. Müller, R. Jansson, A. Elfwing, G. Askarieh, R. Karlsson, M. Hamedi, A. Rising, J. Johansson, O. Inganäs and M. Hedhammar, *J. Mater. Chem.*, 2011, **21**, 2909–2915.
20 C. Müller, M. Hamedi, R. Karlsson, R. Jansson, R. Marcilla, M. Hedhammar and O. Inganäs, *Adv. Mater.*, 2011, **23**, 898–901.
21 M. Hamedi, R. Forchheimer and O. Inganäs, *Nat. Mater.*, 2007, **6**, 357–362.
22 G. Tarabella, M. Villani, D. Calestani, R. Mosca, I. Salvatore, Z. Zappettini and N. Coppedè, *J. Mater. Chem.*, 2012, **22**, 23830–23834.
23 N. Coppedè, G. Tarabella, M. Villani, D. Calestani, I. Salvatore and Z. Zappettini, *J. Mater. Chem. B*, 2014, **2**, 5620–5626.
24 L. Zhang, Y. Yu, G. P. Eyer, G. Suo, L. A. Kozik, M. Fairbanks, X. Wang and T. L. Andrew, *Adv. Mater. Technol.*, 2016, 1600147.
25 M. E. Alf, A. Asatekin, M. C. Barr, S. H. Baxamusa, H. Chelawat, G. Ozaydin-Ince, C. D. Petruczok, R. Sreenivasan, W. E. Tenhaeff, N. J. Trujillo, S. Vaddiraju, J. Xu and K. K. Gleason, *Adv. Mater.*, 2010, **22**, 1993–2027.
26 D. Bhattacharyya, R. M. Howden, D. C. Borrelli and K. K. Gleason, *J. Polym. Sci., Part B: Polym. Phys.*, 2012, **50**, 1329–1351.
27 W. E. Tenhaeff and K. K. Gleason, *Adv. Funct. Mater.*, 2008, **18**, 979–992.
28 K. M. Vaeth and K. F. Jensen, *Adv. Mater.*, 1999, **11**, 814–820.

29 K. K. S. Lau and K. K. Gleason, *Macromolecules*, 2006, **39**, 3688–3694.
30 L. Zhang, M. Fairbanks and T. L. Andrew, *Adv. Funct. Mater.*, 2017, DOI: 10.1002/adfm.201700415.
31 K. L. Choy, *Prog. Mater. Sci.*, 2003, **48**, 57–170.
32 W. E. Tenhaeff and K. K. Gleason, *Adv. Funct. Mater.*, 2008, **18**, 979–992.
33 S. E. Atanasov, M. D. Losego, B. Gong, E. Sachet, J.-P. Maria, P. S. Williams and G. N. Parsons, *Chem. Mater.*, 2014, **26**, 3471–3478.
34 L. Dall'Acqua, C. Tonin, A. Varesano, M. Canetti, W. Porzio and M. Catellani, *Synth. Met.*, 2006, **156**, 379–386.
35 S. Shang, X. Yang, X. Tao and S. S. Lam, *Polym. Int.*, 2010, **59**, 204–211.
36 T. Bashir, M. Ali, S.-W. Cho, N.-K. Persson and M. Skrifvars, *Polym. Adv. Technol.*, 2013, **24**, 210–219.
37 A. Laforgue and L. Robitaille, *Macromolecules*, 2010, **43**, 4194–4200; A. Laforgue, *J. Mater. Chem.*, 2010, **20**, 8233–8235.
38 T. Bashir, M. Skrifvars and N.-K. Persson, *Polym. Adv. Technol.*, 2012, **23**, 611–617.
39 T. Bashir, J. Naeem, M. Skrifvars and N.-K. Persson, *Polym. Adv. Technol.*, 2014, **25**, 1501–1508.
40 P. Kovacik, G. del Hierro, W. Livernois and K. K. Gleason, *Mater. Horiz.*, 2015, **2**, 221–227.
41 S. Sadki, P. Schottland, N. Brodie and G. Sabouraud, *Chem. Soc. Rev.*, 2000, **29**, 283–293.
42 S. Subianto, G. W. Will and S. Kokot, *Int. J. Polym. Mater.*, 2005, **54**, 141–150.
43 S. N. Bhadani, M. Kumari, S. K. Sen Gupta and G. C. Sahu, *J. Appl. Polym. Sci.*, 1997, **64**, 1073–1077.
44 J. Molina, A. I. del Río, J. Bonastre and F. Cases, *Eur. Polym. J.*, 2009, **45**, 1302–1315.
45 J. Molina, A. I. del Río, J. Bonastre and F. Cases, *Eur. Polym. J.*, 2008, **44**, 2087–2098.
46 S. Y. Severt, N. A. Ostrovsky-Snider, J. M. Leger and A. R. Murphy, *ACS Appl. Mater. Interfaces*, 2015, **7**, 25281–25288.
47 A. Maziz, A. Concas, A. Khaldi, J. Stålhand, N.-K. Persson and E. W. H. Jager, *Sci. Adv.*, 2017, **3**, e1600327.
48 C. Das, B. Jain and K. Krishnamoorthy, *Chem. Commun.*, 2015, **51**, 11662–11664.
49 J. Molina, A. I. del Río, J. Bonastre and F. Cases, *Synth. Met.*, 2010, **160**, 99–107.
50 K. Hong, K. Oh and T. Kang, *J. Appl. Polym. Sci.*, 2005, **97**, 1326–1332.
51 A. Varesano, A. Aluigi, L. Florio and R. Fabris, *Synth. Met.*, 2009, **159**, 1082–1089.
52 J. Xu, D. Wang, L. Fan, Y. Yuan, W. Wei, R. Liu, S. Gu and W. Xu, *Org. Electron.*, 2015, **26**, 292–299.
53 A. Akşit, N. Onar, M. Ebeoglugil, I. Birlik, E. Celik and I. Ozdemir, *J. Appl. Polym. Sci.*, 2009, **113**, 358–366.
54 N. Maráková, P. Humpolíček, V. Kašpárková, Z. Capáková, L. Martinková, P. Bober, M. Trchová and J. Stejskal, *Appl. Surf. Sci.*, 2017, **396**, 169–176.
55 (*a*) C. Merlini, G. M. de Oliveira Barra, S. D. A. da Silva Ramoa, G. Contri, R. dos Santos Almeida, M. A. d'Avila and B. G. Soares, *Front. Mater.*, 2015, **2**, 14; (*b*) A. Sarvi, A. B. Silva, R. E. S. Bretas and U. Sundararaj, *Polym. Int.*, 2015, **64**, 1262–1267; (*c*) B. Ding, M. Wang, X. Wang, J. Yu and G. Sun, *Mater. Today*, 2010, **13**, 16–27.
56 W. Ye, J. Zhu, X. Liao, S. Jiang, Y. Li, H. Fang and H. Hou, *J. Power Sources*, 2015, **299**, 417–424.
57 B. Sun, T. Wu, J. Wang, D. Li, J. Wang, Q. Gao, M. A. Bhutto, H. El-Hamshary, S. S. Al-Deyab and X. Mo, *J. Mater. Chem. B*, 2016, **4**, 6670–6679.
58 C. Wu, T. Kim, T. Guo and F. Li, *Nano Energy*, 2017, **32**, 367–373.
59 Y. Guo, M. T. Otley, M. Li, X. Zhang, S. K. Sinha, G. M. Treich and G. A. Sotzing, *ACS Appl. Mater. Interfaces*, 2016, **8**, 26998–27005.
60 A. Scott, *Chem. Eng. News*, 2015, 18–19.
61 N. Cheng, L. Zhang, J. J. Kim and T. L. Andrew, *J. Mater. Chem. C*, 2017, DOI: 10.1039/C7TC00293A.

